Chemosphere 172 (2017) 363–372

Contents lists available at ScienceDirect

Chemosphere

journal homepage: www.elsevier.com/locate/chemosphere

Current ambient concentrations of ozone in Panama modulate the leaf chemistry of the tropical tree *Ficus insipida*

Gerald F. Schneider [a, *], Alexander W. Cheesman [b], Klaus Winter [c], Benjamin L. Turner [c], Stephen Sitch [d], Thomas A. Kursar [a, c]

[a] Department of Biology, University of Utah, 257 South 1400 East, Salt Lake City, UT 84112, USA
[b] College of Science & Engineering, James Cook University, Cairns, Queensland, 4870, Australia
[c] Smithsonian Tropical Research Institute, Apartado 0843-03092, Balboa, Ancon, Panama
[d] Department of Geography, College of Life and Environmental Sciences, University of Exeter, Exeter EX4 4RJ, United Kingdom

HIGHLIGHTS

- Elevated [O_3] was recorded at three forests near NO_x emission hotspots in Panama.
- This [O_3] affected the physiology of the widespread native tree *Ficus insipida*.
- The effects of O_3 on *F. insipida* included a decrease in leaf chemical defenses.
- O_3 also led to decreased lipid content in mature leaves.
- AOT was below critical levels for temperate trees, but *F. insipida* has high g_{s_max}.

ARTICLE INFO

Article history:
Received 24 October 2016
Received in revised form
17 December 2016
Accepted 21 December 2016
Available online 27 December 2016

Handling Editor: R Ebinghaus

Keywords:
Ozone
Tropical forest
Open-top chamber
Secondary metabolite
Senescence
Stomatal conductance

ABSTRACT

Tropospheric ozone (O_3) is a major air pollutant and greenhouse gas, affecting carbon dynamics, ecological interactions, and agricultural productivity across continents and biomes. Elevated [O_3] has been documented in tropical evergreen forests, the epicenters of terrestrial primary productivity and plant-consumer interactions. However, the effects of O_3 on vegetation have not previously been studied in these forests. In this study, we quantified ambient O_3 in a region shared by forests and urban/commercial zones in Panama and found levels two to three times greater than in remote tropical sites. We examined the effects of these ambient O_3 levels on the growth and chemistry of seedlings of *Ficus insipida*, a regionally widespread tree with high stomatal conductance, using open-top chambers supplied with ozone-free or ambient air. We evaluated the differences across treatments in biomass and, using UPLC-MS-MS, leaf secondary metabolites and membrane lipids. Mean [O_3] in ambient air was below the levels that induce chronic stress in temperate broadleaved trees, and biomass did not differ across treatments. However, leaf secondary metabolites – including phenolics and a terpenoid – were significantly downregulated in the ambient air treatment. Membrane lipids were present at lower concentrations in older leaves grown in ambient air, suggesting accelerated senescence. Thus, in a tree species with high O_3 uptake via high stomatal conductance, current ambient [O_3] in Panamanian forests are sufficient to induce chronic effects on leaf chemistry.

1. Introduction

Tropospheric ozone (O_3) is a major globally relevant secondary air pollutant and greenhouse gas, and has a suite of adverse effects on plant growth and physiology. Ozone forms naturally as a product of photochemical reactions with the precursors NO_x, CH_4, CO, and volatile organic compounds (VOCs). Over the industrial period, anthropogenic emissions of these precursors from fossil fuel and biomass burning have increased ambient tropospheric O_3 concentrations over a large portion of the Earth's surface (Vingarzan, 2004). As a secondary air pollutant, O_3 is often present at high concentrations in VOC-emitting vegetated areas that are downwind

* Corresponding author.
E-mail address: gerald.schneider@utah.edu (G.F. Schneider).

http://dx.doi.org/10.1016/j.chemosphere.2016.12.109
0045-6535/

from sources of NO_x precursors. Thus, tropospheric O_3 has become a global air pollutant: many regions are already experiencing near-surface O_3 concentrations that can cause visible plant damage and/or reduce primary productivity in natural and agricultural ecosystems (Sandermann, 1996; Fuhrer et al., 1997; Chappelka and Samuelson, 1998; Skarby et al., 1998; Fowler et al., 1999; Vingarzan, 2004; Mills et al., 2011a,b; Ainsworth et al., 2012). Further, regional and global models have forecasted near-surface O_3 concentrations to reach two to eight times their pre-industrial levels by the year 2100 (Fowler et al., 1999; Vingarzan, 2004; Wild et al., 2012; Naik et al., 2013), with the potential to significantly reduce the land carbon sink and thus contribute to climate warming (Sitch et al., 2007).

The influence of O_3 on plants has generally been assessed on the basis of reductions in plant growth and productivity (Ashmore, 2005). Ozone generates reactive oxygen species and causes oxidative stress within leaves, which in turn decreases photosynthesis, plant growth, and biomass accumulation (reviewed by e.g. Skarby et al., 1998; Chappelka and Samuelson, 1998; Karnosky et al., 2007; Ainsworth et al., 2012). Early experiments on the impacts of O_3 on herbaceous crop species led to an adoption of $[O_3] = 40$ ppb as an approximate threshold, or critical level, for adverse effects on plant productivity. However, it was subsequently recognized that this critical level varies widely among plant species and even among genotypes within species, due mainly to differences in stomatal conductance and thus differences in the flux of O_3 into the leaf at a given value of ambient $[O_3]$ (reviewed by Fuhrer et al., 1997; Chappelka and Samuelson, 1998; Musselman et al., 2006; Karnosky et al., 2007; Mills et al., 2011a; Ainsworth et al., 2012; Anav et al., 2016). A key finding from these studies is that stomatal conductance and $[O_3]$ both exhibit a linear relationship to leaf-level O_3 dose (dose $\propto g_s * [O_3]$). Consequently, plant biomass or photosynthesis reductions in response to O_3 are generally correlated more strongly with cumulative O_3 uptake than with accumulated O_3 exposure (reviewed by Karlsson et al., 2004; Büker et al., 2015). In addition to stomatal conductance, the leaf-level capacity for detoxification of reactive oxygen species also plays a role in determining the critical level for a species or genotype.

Although tropospheric O_3 is a global air pollutant, its effects on plant productivity and trophic interactions have mainly been studied in temperate regions of the northern hemisphere. This is despite the potential for elevated $[O_3]$ to have deleterious impacts on plant productivity and the tropical carbon cycle (Pacifico et al., 2015). In forested regions of the tropics, numerous monitoring campaigns have already studied $[O_3]$ at and near the atmosphere-biosphere interface (Kaplan et al., 1988; Fan et al., 1990; Jacob and Wofsy, 1990; Kirchhoff et al., 1990; Cros et al., 1992, 2000; Andreae et al., 2002; Gut et al., 2002; Rummel et al., 2007; Karl et al., 2009; Jardine et al., 2011; Andreae et al., 2015). During the LBA-EUSTACH project (Rummel et al., 2007), $[O_3]$ within the forest canopy exceeded 40 ppb, the exposure-based critical level for many temperate plant species (reviews by Fuhrer et al., 1997; Chappelka and Samuelson, 1998).

Modeling efforts over the past decade have explored the ramifications of elevated O_3 on tropical forest ecosystems. Sitch et al. (2007) simulate a large negative impact of projections of increasing O_3 concentrations on the tropical carbon sink. In addition, Pacifico et al. (2015) were able to reproduce the Rummel et al. (2007) deposition velocities in an Earth System Model, and thus we have confidence in the ability to simulate the O_3 flux into leaves. However, these global modeling efforts rely on dose response relationship based on temperate and boreal species (Sitch et al., 2007; Pacifico et al., 2015). Few studies have investigated the effects of O_3 pollution on tropical tree species (Cassimiro and Moraes, 2016; Furlan et al., 2008), and with notable exceptions (Assis et al., 2015) little work has been done in integrating leaf-physiology and exposure levels to determine critical levels for adverse effects in tropical tree species. The main leaf-level physiological determinants of a plant species' O_3 critical level are detoxification capacity and stomatal flux (Karlsson et al., 2004; Musselman et al., 2006; Mills et al., 2011b; Büker et al., 2015). Evaluations of leaf-level detoxification capacity have not been conducted for tropical trees, but stomatal flux data have been collected from an array of species (Zotz and Winter, 1996; Poorter and Bongers, 2006). For trees of tropical lowland moist forests, maximal stomatal conductance is approximately 85% higher than that for temperate deciduous trees (Kelliher et al., 1995; Körner, 1995; Poorter and Bongers, 2006), suggesting that many species of tropical trees may be sensitive to O_3 pollution given the linear relationship between stomatal conductance and O_3 dose.

In addition to its well-characterized effects on plant physiology, O_3 pollution can influence plant chemical defenses against biotic and abiotic stressors (reviewed by Sandermann, 1996; Kangasjärvi et al., 2005; Valkama et al., 2007; Bidart-Bouzat and Imeh-Nathaniel, 2008; Lindroth, 2010). After O_3 is taken up through the stomata, O_3 and O_3-generated reactive oxygen species (ROS) activate hormones involved in all major defense signaling pathways, including ethylene, abscisic acid, jasmonic acid, and salicylic acid. The activation of these hormones influences the synthesis of secondary metabolites, which can in turn alter the dynamics of plant-herbivore interactions. Available data suggest that the dose-responses of secondary metabolic pathways to O_3 vary in magnitude and direction across types of secondary metabolites, plant developmental stage, and plant and herbivore species (Valkama et al., 2007; Lindroth, 2010). While these effects of O_3 uptake on secondary metabolic pathways have been noted in conjunction with the aforementioned effects on primary physiology in many studies of chronic low-level O_3 exposure, it is not known whether these two types of effects share a critical level.

The present study is motivated by considering the potential impacts of O_3 on the contribution of tropical forest primary productivity to the global carbon budget, as well as on the plant-consumer interactions integral to tropical forest biodiversity. Satellite-based measurements and modeling of emissions have indicated a hotspot of NO_x (precursors to O_3) in Panama, specifically within the region surrounding the Panama Canal and Panama City (Hietz et al., 2011). We conducted the present study to measure O_3 concentrations within forested areas surrounding this hotspot of O_3-precursors and to investigate the effects of ambient O_3 concentrations in Panama on a common species of tropical tree. Our research questions are: 1) how do O_3 concentrations vary across the Pacific-Caribbean gradient of forests within the Panama Canal watershed, 2) how do O_3 concentrations vary across the forest strata, from the canopy to the understory, within a given site, and 3) for a tropical tree species with relatively high stomatal conductance, does exposure to ambient concentrations of O_3 in the Panama Canal watershed impact primary productivity, secondary metabolic pathways, and/or leaf senescence? To address these questions, we conducted an O_3 monitoring campaign at four sites over two years and an open-top chamber experiment with potted tree seedlings.

2. Materials and methods

2.1. Regional O_3 monitoring

Since tropospheric $[O_3]$ had not previously been measured in the vicinity of the Panama Canal and surrounding urban areas, and precursor emissions were known to be present (Hietz et al., 2011), we conducted monitoring to assess the distribution of O_3 across

and within forested areas in this region (Fig. 1). Three monitoring sites were selected based on their proximity to precursor sources. These sites included Santa Cruz Experimental Field Facility (SCEFF), Barro Colorado Island (BCI), and Parque Natural Metropolitano (PNM). SCEFF, operated by the Smithsonian Tropical Research Institute, is located approximately 800 m from the Panama Canal in an open area on the outskirts of the town of Gamboa, adjoining secondary moist forest with a canopy height of 20–30 m. Gamboa is located approximately 25 km northwest of Panama City. BCI comprises 1560 ha of lowland moist forest with a canopy height of 20–40 m (Leigh et al., 1996), situated amid the Panama Canal 40 km northwest of Panama City. Our study sites on BCI are between 500 m and 1 km from the Panama Canal. PNM comprises 265 ha of lowland dry forest with a canopy height of 25–35 m (STRI Physical Monitoring Program, 2016) and is located within the limits of Panama City approximately 4 km from the Panama Canal. Monitoring at SCEFF was conducted in two locations, 1) in a grass-dominated clearing (grass height <20 cm), hereafter referred to as grassy clearing, next to the open-top chamber experiment described below and 2) at a height of 1 m in the forest understory at the edge of the facility, ~10 m into the forest from its edge. At BCI, O_3 was measured using a UV-absorbance monitor and passive samplers. For the latter, O_3 measurements were taken at three locations: 1) at a height of 1 m in a tree fall gap with a layer of broadleaved vegetation <1 m tall, along the trail to the Lutz observation tower ~500 m inland from the Panama Canal, 2) at a height of 1 m adjacent to the Lutz observation tower within closed-canopy forest, and 3) at a height of 48 m atop the Lutz tower, approximately 12 m above the surrounding canopy. The UV-absorbance monitor was located at 48 m on the Lutz tower ("location #3"). At PNM, measurements were taken at three locations in the forest: 1) approximately 12 m above the surrounding canopy on a 42 m tall canopy access crane operated by the Smithsonian Tropical Research Institute, 2) at a height of 1 m the base of this canopy crane, and 3) at a height of 1 m in a tree fall gap with a layer of broadleaved vegetation <1 m tall, ~100 m from the canopy crane. While the tree fall gaps at BCI and PNM and the grassy clearing at SCEFF differed in vegetation type, we grouped them for analysis based on their similar environmental contrasts to nearby forested areas.

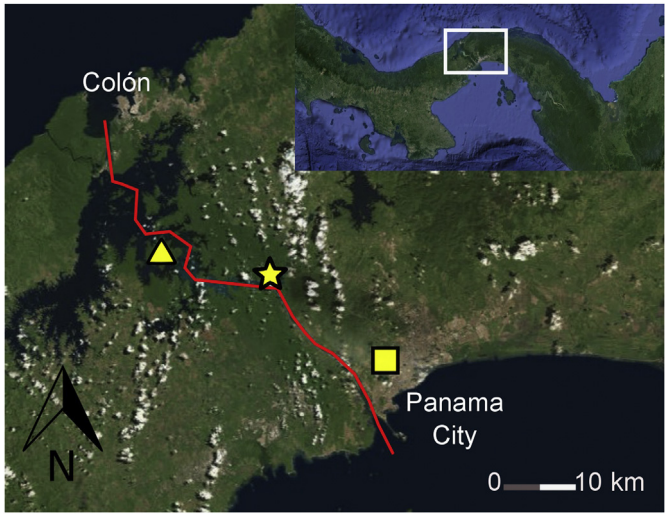

Fig. 1. Map of the Republic of Panamá and study sites. The outlined area in the inset map indicates the area covered by the study site map. The Panama Canal channel is indicated by a solid line drawn between the cities of Colón and Panama City. Barro Colorado Island (BCI) is indicated by a triangle; Santa Cruz Experimental Field Facility (SCEFF) is indicated by a star; Parque Natural Metropolitano (PNM) is indicated by a square. Map data © Google 2016.

Monitoring equipment consisted of a Model 205 UV-absorbance type monitor (2B Technologies, Boulder, CO) and eight passive samplers (Ogawa & Co., Pompano Beach, FL). The Model 205 monitor recorded data at BCI location #3 during the dry and wet seasons of 2013 and 2014, starting in April 2013. The monitor recorded the running mean of [O_3] every 10 min. The monitor was calibrated by 2B Technologies immediately prior to deployment. The data recorded by this monitor include a total of 207 days and meet or exceed in duration some data from other tropical sites (see Discussion). Our data were collected periodically in order to reflect multiple seasons and years, minimizing the influence of short-term environmental perturbations or fluctuations.

The passive samplers were stationed at SCEFF locations #1-2, BCI locations #1-3, and PNM locations # 1-3 from 21 January – 19 March 2015, with one sampler at each location, for a total of 8 samplers. Passive sampling pads were exchanged every 14 days, for a total of four pads per sampler over the course of the campaign. To control for the background reaction rates of the sampling pads, pads in sealed opaque containers were placed alongside exposed pads at all locations. Passive sampling pads were analyzed via ion chromatography at RTI International (Research Triangle Park, NC), using the protocol recommended by Ogawa & Co.

From the Model 205's raw data, we calculated hourly mean [O_3], daytime (7:00–17:00) mean [O_3], daytime peak [O_3], and daytime (7:00–17:00) accumulated [O_3] (AOTX). Daytime AOTX, or Accumulated O_3 over a Threshold of Xppb, is the daily sum of all hourly mean O_3 concentrations greater than Xppb. Unlike mean [O_3], AOTX accounts for duration of exposure to elevated [O_3], and when X is the critical level for a given plant species or genotype, AOTX generally exhibits a stronger correlation than mean [O_3] with plant responses to O_3 (Fuhrer et al., 1997). As critical levels have not been identified for any tropical tree species, we calculated AOTX using $X = 10$ and $X = 20$, approximately 1/3 and 2/3 of the observed maximum [O_3] at SCEFF (29.6 ppb). We conducted statistical analyses of data from the 2B Technologies monitors using the mean from a single day as one replicate for each location/site. We assessed the normality of the data using a Shapiro-Wilk test. The test indicated that the data did not differ significantly from a normal distribution, and we proceeded with analyses using parametric tests. We then compared the daytime means at each location to one another using two-way ANOVA and pairwise t-tests. All statistical analyses were conducted in R© v 3.1.3 (R Core Team, 2015).

For the passive sampler data, we used a mixed-effects linear model with time as a random effect and site and vertical stratum as fixed effects. To construct this model, we used the packages "lme4" and "lmerTest" in R© v 3.1.3 (R Core Team, 2015).

2.2. Open-top chamber experiment

2.2.1. Tree growth and harvest

We studied the fast-growing, early-successional tree *Ficus insipida* Willd. (Moraceae). This species occurs throughout the Neotropics, from lowland forest to cloud forest and from dry forest to wet forest (Tropicos.org, 2016). In the moist lowland area where the experiment was conducted, naturally occurring *F. insipida* are evergreen. *F. insipida* has high maximum stomatal conductance, 750 ± 80 mmol m^{-2} s^{-1}, as measured in growth conditions similar to those of the present study (Cernusak et al., 2007). Seeds were collected from trees growing at <50 m a.m.s.l. within forests surrounding Panama City and germinated in seed-tray flats in a ventilated screen-house (70% natural sunlight) at the SCEFF. After emergence of cotyledons at least three seedlings were transplanted

into each experimental pot, with a total of 24 pots per O_3 treatment. Pots were 1.75 l in volume (TP-49 Treepot™, Stuewe & Sons, Tangent, OR), containing a non-sterilized mix of native top soil and 20% (by volume) vermiculite used to improve soil structure. Seedlings were left under standard conditions for 2 weeks prior to thinning to one seedling per pot and initiation of the experiment. Upon initiation of the experiment, pots were randomly assigned to open-top chambers, with eight pots assigned to each chamber.

Six open-top chambers were established at SCEFF, each consisting of a PVC frame (volume of 2.2 m^3) with lower chamber walls of reflective insulation and an upper portion (150 cm) of clear polyethylene film. Ventilation was provided by six independent fans (TD-150; Soler &Palau, Jacksonville, FL) drawing ambient air from a shaded site and delivered via a PVC conduit to a distribution point at the center of each chamber. Three of the chambers drew their air through an activated charcoal air filter 150 × 500 mm (LEDwholesalers, CA, USA) which when spot-checked at midday reduced O_3 in the airstream of the fans to below the detection limit (2.0 ppb). Thus, we considered [O_3] in the filtered air treatment to be effectively zero. We refer to this as the ozone-free treatment. Activated charcoal filtering has been used in numerous studies to provide an ozone-free or low ozone control treatment to evaluate the effects of ambient [O_3] on vegetation (summarized in Wittig et al., 2009; Büker et al., 2015). Although activated charcoal also removes many other air pollutants, we conclude that the leaf chemical responses we observed are due to O_3 based on their congruence with leaf chemical responses to O_3 in other species, as addressed in the discussion section.

Seedlings were grown under experimental conditions for 50 days before harvest, 21 December 2012–3 February 2013. At harvest roots were inspected to verify that they had not become pot-bound, and none had become so. Plants were then separated into leaf-lamina, stem + petioles, and roots. Leaf area of both the most recent fully expanded leaf and total leaf area was determined using a Li-3100 leaf area meter (Li-Cor, Lincoln, NE). The roots were separated from soil by hand sorting, dry sieving and washing. All samples were dried to constant mass at 70 °C and weighed. Biomass and leaf area data were used to calculate total biomass accumulation and, leaf mass per area (LMA g m^{-2}) of all leaves and the most recent fully expanded leaf.

Ambient O_3 concentrations were monitored at SCEFF over the latter 33 of the 50 experimental days; technical faults prevented measurements over the preceding days. Ozone concentrations were determined using a 2B Technologies Model 205 O_3 monitor identical to that used in the regional monitoring portion of the study. The O_3 monitor sampled from a shaded, yet not sheltered, position at ~1.5 m above grass.

Biomass accumulation/allocation was analyzed within species using a *t*-test of the chamber mean (n = 3) of the 8 replicate plants. The mean and interquartile range were calculated for [O_3] during daylight hours (7:00–17:00). All statistics and graphical operations were carried out using R© v 3.2.3 (R Core Team, 2015).

2.2.2. Leaf secondary metabolites

Analyses of secondary metabolite content were conducted using dried leaf material. For these analyses, we collected the youngest (≤1 week since full expansion) and second-youngest fully expanded leaves, referred to hereafter as “younger” and “older” leaves. As secondary metabolite content is known to change quantitatively and qualitatively across leaf ontogeny, we analyzed younger and older leaves separately. Upon collection, leaves were stored on ice in a portable cooler and brought to the laboratory at Barro Colorado Island for drying. Drying was initiated no more than 2 h after leaf collection. Drying was conducted at room temperature (~22 °C) for 72 h under high vacuum. Only individuals with recently expanded leaves were sampled. As a result, a subset of plants (n = 6; 2 per chamber) was analyzed for secondary metabolites and membrane lipids. Dried leaf samples were transported to the University of Utah for analyses via ultra-performance liquid chromatography – mass spectrometry (UPLC-MS) and tandem mass spectrometry (MS-MS). Samples were prepared and analyzed according to the methods in Wiggins et al. (2016), as summarized in the following paragraphs, with the exception of the extraction procedure: The leaf extract was collected in two fractions for analysis: 1) an intermediate polarity fraction containing compounds such as phenolics and saponins, extracted with 50% aqueous acetonitrile, and 2) non-polar compounds such as non-oxygenated terpenes and lipids, extracted with a series of 100% acetonitrile, 100% methanol, and 100% acetone.

Using the net weights of the leaf extract fractions, we conducted a quantitative analysis comparing weights between leaves from the two treatments. These gravimetric comparisons were conducted separately for the two leaf extract fractions. We assessed the normality of the data from each comparison using Shapiro-Wilk tests. The tests indicated that the data did not differ significantly from a normal distribution, and we proceeded with analyses using parametric tests. We performed unpaired, two-tailed Student's t-tests for each extract fraction × leaf age comparison. These analyses were conducting using R© v 3.1.3 (R Core Team, 2015).

The intermediate polarity fraction, containing phenolics and terpenoids, was analyzed via UPLC-MS and MS-MS as in Wiggins et al. (2016). The nonpolar fraction was analyzed via UPLC-MS and MS-MS at the Metabolomics Core Facility at the University of Utah. The instruments used were an Agilent® 1290 Infinity LC system (Agilent Technologies, Santa Clara, CA) with an Acquity® UPLC CSH C18 1.7 μm (2.1 × 100 mm) column (Waters) and an Agilent 6520 Q-ToF mass spectrometer with dual electrospray ionization sources.

Next, we compared relative abundances of putative compounds appearing in the UPLC-MS analyses. In order to identify and then align features present in multiple samples, CDF data files were processed using XCMS and CAMERA (Bioconductor v3.1 (Smith et al., 2006; Tautenhahn et al., 2008; Benton et al., 2010; Kuhl et al., 2012) in R v3.1.3 (R Development Core Team, 2015). The CAMERA tool in this software was used to combine mass spectral features generated by XCMS into putative compounds. The XCMS output was inspected manually to ensure that isotopic peaks and adducts were combined with parent ions as putative compounds, hereafter referred to as “compounds”. To test whether secondary metabolite suites segregated by experimental treatment, we used MetaboAnalyst 3.0 (Xia et al., 2015) to perform partial least-squares discriminant analyses (PLS-DA) on the compound tables. XCMS was then used to compare normalized TICs for each compound using unpaired two-tailed Welch t-tests. Compounds exhibiting significant differences between treatments at $P < 0.05$ were compared to the METLIN database using accurate masses from our MS data, and we accepted matches of ≤10 ppm mass difference as putative compounds. In conjunction with METLIN searches, we compared our empirical tandem-MS fragmentation spectra with predicted fragmentation spectra from CFM-ID (Competitive Fragmentation Modeling for Metabolite Identification; Allen et al., 2015) to assign putative identifications to features based on matching fragmentation patterns.

For the nonpolar fraction, we used MassHunter (Agilent Technologies) to consolidate features from the raw UPLC-MS output data. After known contaminants were removed from the data, the

data were analyzed in R© version 3.1.3 (R Core Team, 2015). TICs for each feature were compared between ambient air and ozone-free air treatments using unpaired two-tailed Welch t-tests. As with the intermediate polarity fraction, we used METLIN and CFM-ID to search for compounds matching the UPLC-MS features. We accepted putative molecular formulas for features if the match probability was ≥90% as calculated by MassHunter.

3. Results

3.1. Regional O_3 monitoring

In comparing equivalent strata across sites using passive samplers, BCI exhibited the highest mean 24 h O_3 concentrations in all strata, followed by PNM and SCEFF (Fig. 2). In the canopy, these means were 21.7 ppb (BCI) and 18.3 ppb (PNM) (Fig. 2). In tree fall gaps and the grassy clearing, these means were 17.7 ppb (BCI), 12.7 ppb (PNM), and 11.2 ppb (SCEFF) (Fig. 2). At the forest floor, these means were 15.7 ppb (BCI), 7.3 ppb (PNM), and 7.2 ppb (SCEFF), with the latter two sites not significantly different from one another (Fig. 2). The passive samplers also indicated that, within all sites, O_3 concentrations were highest at canopy level, intermediate at ground-level in tree fall gaps and the grassy clearing, and lowest at the forest floor under closed canopy (Fig. 2). The O_3 concentration declined by an average of 24.5% from canopy to tree fall gap and grassy clearing, by 44% from canopy to forest floor, and by 47.4% from tree fall gap and grassy clearing to forest floor (Fig. 2). The largest declines across strata were found at PNM, followed by SCEFF and BCI (Fig. 2).

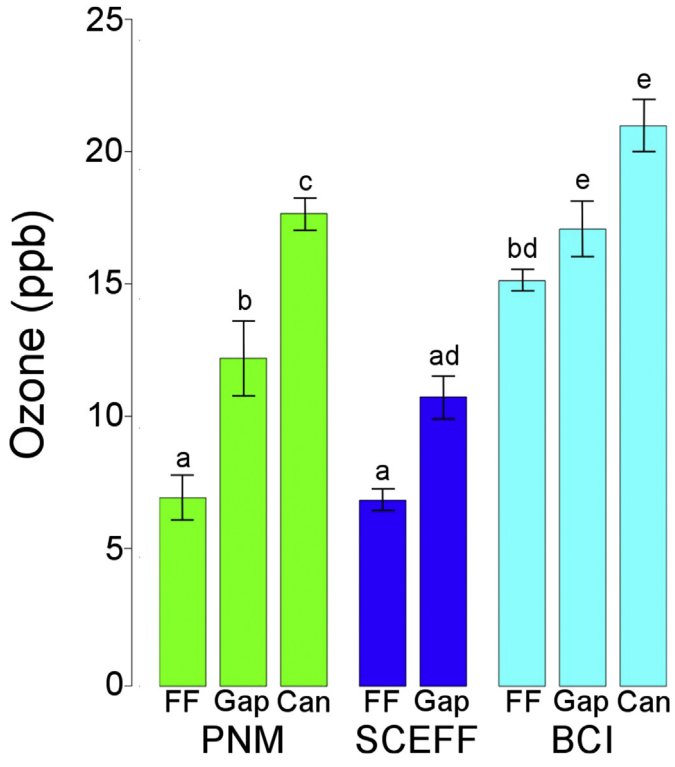

Fig. 2. Passive sampler monitoring. Mean 24hr $[O_3]$ ± SEM in forest floor (FF), tree fall gap or grassy clearing (Gap; tree fall gaps at PNM and BCI, grassy clearing at SCEFF), and canopy (Can) strata indicated by passive sampling at Parque Natural Metropolitano (PNM), Santa Cruz Experimental Field Facility (SCEFF), and Barro Colorado Island (BCI), 22 January – 19 March 2015. n = 4 sampling pads per sampler. Statistically significant differences at $p \leq 0.05$ across strata and sites are indicated by different letters above the bars.

In examining daily patterns in $[O_3]$ using the Model 205 UV-absorbance monitor above the canopy at BCI (48 m above the forest floor), we found that $[O_3]$ increased during daytime to a midday (13:00–15:00) peak 1.5- to 2-fold above the pre-dawn $[O_3]$, subsequently declining steadily until 22:00–24:00 (Fig. S1). Also at this location, the inter-seasonal and inter-annual comparisons of O_3 using the Model 205 indicated a trend towards higher daytime means of $[O_3]$ and AOT10 in the dry season (Table 1). The highest $[O_3]$ and AOT10 were observed in the dry season of 2014 (24.4 ppb and 143.7 ppb h) and the lowest in the wet season of 2014 (18.4 ppb and 82.7 ppb h) (Table 1).

3.2. Open-top chamber experiment

Over the 50 days of experimental growth, seedlings showed only minor differences ($P > 0.05$) in biomass and leaf area between treatments (Table 2). Daytime $[O_3]$ in ambient air averaged 17.6 ppb, with a maximum of 29.6 ppb and 50% of measurements falling between 14.7 and 22.5 ppb (Fig. S1). Daytime accumulated O_3 exposure above 10 ppb (AOT10, see methods) averaged 70.6 ppb, and AOT20 averaged 6.4 ppb. Ozone concentration in the filtered treatment was below detection limits when spot checked at midday. Thus, $[O_3]$ in the filtered treatment was regarded as effectively zero and AOT10 was zero.

For both leaf age classes, the dry weight of the intermediate polarity fractions, which contained secondary metabolites such as phenolics and terpenoids, did not differ significantly across O_3 treatments. However, analysis of these fractions via chromatography and mass spectrometry indicated that the concentrations of ten compounds changed significantly ($P < 0.05$) and by ≥ 1.5 fold across treatments for both leaf age classes (Table 3; Fig. 3). Of the ten O_3-responsive compounds, five were in fractions from younger leaves and five were in fractions from older leaves, with no compounds overlapping across leaf age classes. All but one of these ten compounds were present at lower concentrations in leaves from the ambient air treatment. PLS-DA also indicated significant clustering ($P < 0.05$) by treatment based on relative abundances of all compounds within the intermediate polarity fractions of both leaf age classes (Fig. 4).

The METLIN database yielded matches for nine of the ten O_3-responsive compounds. For these, eight of the MS^2 spectra predicted by CFM-ID matched one or more diagnostic fragments in our observed MS^2 spectra (Table S1). Based on the fragmentation spectra, these eight compounds fell into the following chemical classes: flavonoids (2), flavonoid glycosides (4), lignan glycoside (1), and terpene glycoside (1) (Table 3). We were not able to obtain empirical fragmentation spectra for the remaining two compounds. For one of these compounds, the METLIN database yielded no matches, and for the other of these two compounds, matches included compounds in three classes: furanocoumarins, sesquiterpene lactones, and lignans.

The gravimetric comparisons of the nonpolar fraction, which contained lipids, indicated no differences across treatments in younger leaves but lower mass in the ambient air treatment in the older leaves (Fig. 5). The analyses of the older leaves indicated that ten compounds differed in concentration across treatments, all of which exhibited a fold-change of ≥1.5 (Table 4). Nine of these were present at lower concentrations in the ambient air treatment. Comparisons of accurate masses to the METLIN database and of MS^2 spectra to the spectra predicted by CFM-ID yielded four matches with diglycerides, one match with a galactolipid, and one match with the molecular formula $C_{43}H_{72}O_{10}$ without a putative structure. No matches were found for the remaining four compounds.

Table 1
Comparisons of inter-annual and dry-vs. wet-season differences in ozone exposure and concentrations above the canopy at BCI location #3. Values for daytime 10-h accumulated O_3 exposure (AOT, see methods) and O_3 concentration are means ± SE. Season-year combinations not sharing letter suffixes were significantly different ($P < 0.05$).

	Dry 2013	Wet 2013	Dry 2014	Wet 2014
Daytime mean [O_3] (ppb) 07:00–17:00	20.7 ± 1.7 a	18.9 ± 1.3 ab	24.4 ± 0.6 c	18.4 ± 0.8 b
Daytime accumulated O_3 > 10 ppb (AOT10 ppb h) 07:00–17:00	106.2 ± 11.5 a	88.2 ± 6.5 ab	143.7 ± 3.6 c	82.7 ± 4.1 b
Daytime accumulated O_3 > 20 ppb (AOT20 ppb h) 07:00–17:00	61.5 ± 15.3 a	29.7 ± 5.9 b	48.2 ± 3.2 ab	27.8 ± 6.3 b
Max [O_3] (ppb)	49.1	51.3	40.5	37.2
Monitoring days	33	49	71	54

Table 2
Biomass and leaf area comparisons across ozone treatments. Values are arithmetic means ± SD calculated from three chamber replicates per treatment, using averages for each chamber previously calculated from values for 8 seedlings per chamber. LMA = leaf mass per area. Asterisks indicate marginally significant treatment effects ($0.05 < P < 0.1$).

	Ambient	Filtered
Root mass (g)*	0.43 ± 0.04	0.35 ± 0.05
Stem mass (g)	0.16 ± 0.01	0.14 ± 0.04
Leaf mass (g)	0.48 ± 0.03	0.40 ± 0.07
Shoot/root mass	1.26 ± 0.05	1.29 ± 0.04
Total Biomass (g)	1.08 ± 0.08	0.89 ± 0.16
Youngest leaf		
Leaf Area (cm^2)*	18.2 ± 0.8	15.8 ± 1.3
LMA (g m^{-2})	59.2 ± 3.4	56.6 ± 1.9
Whole seedling		
Leaf Area (cm^{-2})	92.6 ± 1.12	79.47 ± 10.91
LMA (g m^{-2})	52.0 ± 2.43	50.55 ± 1.94

4. Discussion

Several studies have documented elevated [O_3] directly above or within tropical forests (Matsuda et al., 2006; Rummel et al., 2007; Gerken et al., 2016). The majority of these studies (Rummel et al., 2007; Gerken et al., 2016) point to biomass burning as the probable cause of this elevated [O_3] (Pacifico et al., 2015). While biomass burning occurs widely in the tropics (Crutzen and Andreae, 1990; Jacob et al., 1996; Fishman et al., 2003; Hietz et al., 2011), our study indicates that emissions from urban areas and from long-range transport can also be sufficient to generate elevated [O_3] in tropical forests. The means of [O_3] that we observed in Panama exceeded those from more remote tropical forests by approximately two-to three-fold (Bakwin et al., 1990; Kirchhoff et al., 1990; Cros et al., 1992; Andreae et al., 2015). This is consistent with modeling from satellite data that is indicative of O_3 hotspots around many urban, industrial, and agricultural centers in the tropics (Emmons et al., 2010). However, the exposure levels we observed (highest daytime mean [O_3] = 24.4 ppb; Table 1) were well below the 30–40 ppb accumulated exposure threshold above which reductions in growth and photosynthesis are assumed to occur in temperate species (reviewed by Fuhrer et al., 1997; Chappelka and Samuelson, 1998; Musselman et al., 2006; Karnosky et al., 2007; Ainsworth et al., 2012). Despite being below this presumed critical threshold and showing only limited impact upon short term seedling growth, our results clearly demonstrate the impact of ambient pollution upon secondary leaf chemistry in the pioneer tree species *Ficus insipida*.

We found that [O_3] at the forest floor was 40%–70% of that in the forest canopy and tree fall gaps, at PNM and BCI respectively. The few published studies reporting on the proportion of [O_3] that reaches the forest floor varies from 10% to 40% of the canopy-level [O_3] (Fan et al., 1990; Cros et al., 1992; Andreae et al., 2002; Rummel et al., 2007; Karl et al., 2009; Andreae et al., 2015). The reasons for variability among sites are unclear but likely involve differences in deposition to and uptake by vegetation, which along with rainfall and boundary layer variation are the primary factors determining vertical profiles of [O_3] within tropical forests (Fan et al., 1990; Andreae et al., 2002). At BCI, the proportion of [O_3] that reaches the forest floor is considerably higher than previously recorded in a comparable forest type, possibly due to the sampling location being sufficiently close to the forest edge to be affected by lateral O_3 diffusion. Vegetation in the forest canopy and in tree fall gaps is most likely to be affected by O_3 at the observed concentrations,

Table 3
Intermediate polarity compounds exhibiting significant ($P < 0.05$) differences in concentration and ≥1.5-fold change across ozone treatments, listed separately for younger and older leaves. A negative fold-change indicates a lower concentration in the ambient vs. the ozone-free treatment. *m/z* indicates the ratio of the mass of the ion in daltons to the total number of charges. [M - H]- indicates that all of the observed ions were the deprotonated molecule and have a charge of −1. n = 6 plants.

m/z ($[M - H]^-$)	*P*-value	Fold-change	Predicted molecular formula ([M])	METLIN match	Classification of compound
Younger leaves					
271.0602	0.031	−1.52	$C_{15}H_{12}O_5$	naringenin	Flavonoid
445.0765	0.014	−1.5	$C_{21}H_{18}O_{11}$	genistein 4′-*O*-glucuronide	Flavonoid glycoside
461.1083	<0.001	−1.55	$C_{22}H_{22}O_{11}$	rhamnetin 3-rhamnoside	Flavonoid glycoside
895.1915	0.014	−1.88	$C_{42}H_{40}O_{22}$	dimer of rhamnetin 3-alpha-L-arabino-furanoside	Flavonoid glycoside
1011.24	0.01	−1.5	n/a	none	n/a
Older leaves					
289.0708	0.01	2.7	$C_{15}H_{14}O_6$	epicatechin	Flavan-3-ol (Flavonoid)
387.2015	0.03	−2.04	$C_{19}H_{32}O_8$	corchoionoside A	Terpene glycoside
417.155	0.006	−1.52	$C_{22}H_{26}O_8$	various	Furanocoumarin, lignan, or sesquiterpene lactone
521.202	0.004	−1.55	$C_{26}H_{34}O_{11}$	(+)-isolarisiresinol 2a-*O*-beta-D-glucopyranoside	Lignan glycoside
799.2077 2″-(6-(E)-ferulyl-glucoside)	0.002 Flavonoid glycoside	−3.24	$C_{38}H_{40}O_{19}$	isoscoparin	

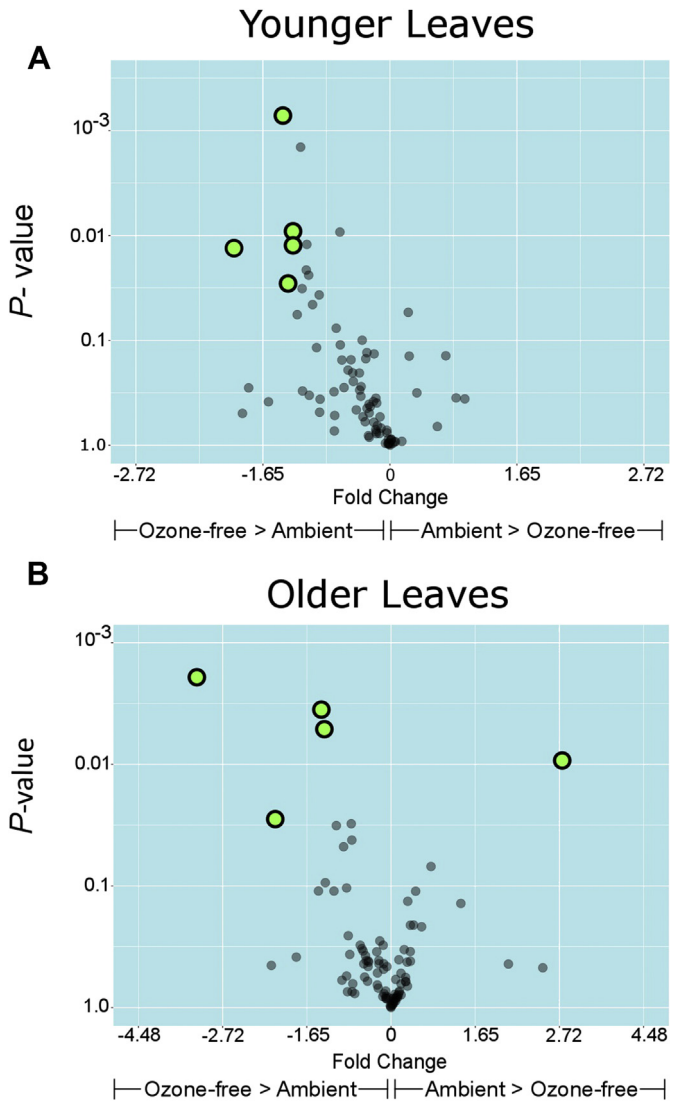

Fig. 3. "Volcano" plots of inter-treatment differences in concentration of compounds in intermediate polarity fraction of (upper panel) younger leaves and (lower panel) older leaves. Each point represents one compound. Compounds exhibiting fold-change $\geq$ 1.5 and statistical significance at $P < 0.05$ are denoted by larger, lightly shaded symbols with dark margins. The Y axis is displayed on a $\log_{10}$ scale and the X axis is displayed on an ln scale. n = 6 plants.

owing to the relatively high stomatal conductance of leaves in those strata (150–570 mmol m^{-2} s^{-1}, (Pearcy, 1987; Roberts et al., 1990; Zotz and Winter 1996; Poorter and Bongers, 2006)), while understory vegetation may be minimally exposed due to stomatal conductances that are up to 8-fold lower (70–150 mmol m^{-2} s^{-1}, (Pearcy, 1987; Roberts et al., 1990)) combined with lower [O_3]. However, leaves in the canopy and in tree fall gaps may close their stomata mid-day (Zotz et al., 1995), while [O_3] is at its peak, potentially mitigating their uptake of O_3.

In the open-top chamber experiment, we observed O_3-associated differences in foliar chemistry that were consistent with effects of chronic O_3 exposure (reviewed by Lindroth, 2010). The upregulation of a flavanol phenolic compound in older leaves in the ambient air treatment mirrors the trend for foliar phenolics in temperate species (Lindroth, 2010). The reduced membrane lipid content of older leaves in the ambient air treatment in comparison to their counterparts in the ozone-free treatment (Fig. 5) is consistent with accelerated leaf senescence (Simon, 1974), a common effect of chronic O_3 exposure. Although we did not measure chlorophyll content, a good measure of senescence, the mass of the nonpolar fraction, containing mainly lipids, decreased by 58% in mature leaves (Fig. 5). This is similar to the magnitude of lipid loss observed during senescence in other species (Mishra et al., 2006; Yang and Ohlrogge, 2009).

To the extent that it may be a functional response, the upregulation of phenolics in response to chronic O_3 uptake is thought to increase the total antioxidant capacity within the leaf. Phenolics exhibit free radical scavenging activity *in vitro* that is comparable to known antioxidant compounds such as α-tocopherol (Krause et al., 2006, 2007), although the necessary enzymatic regeneration process for efficient radical scavenging by phenolics *in vivo* has yet to be identified. Aglycone phenolics exhibit higher antioxidant activity *in vitro* than phenolic glycosides (Hopia and Heinonen, 1999) which, if phenolics do function as radical scavengers *in vivo,* could help explain the simultaneous downregulation of the four flavonoid glycosides with upregulation of the aglycone flavan-3-ol in the ambient air treatment of *F. insipida* (epicatechin, Table 3). Downregulation of phenolic glycosides in response to chronic O_3 exposure has also been observed in aspen (*Populus tremuloides* Michaux.) (Kopper and Lindroth, 2003).

As flavonoid glycosides often function in defense against herbivory, their downregulation along with that of the other secondary metabolites we have described could lead to an increase in herbivory rates. An example of this is available from a temperate forest, where an 11% reduction of foliar phenolics in *Populus tremuloides* exposed to elevated O_3 resulted in a 12–15% decrease in larval development time and 31% increase in pupal mass for the lepidopteran herbivore *Malacosoma disstria* (Kopper and Lindroth, 2003). Thus, one important ecological effect of O_3 in tropical systems could be changes in herbivore performance in the context of altered plant secondary metabolite content.

In the ambient air treatment of our open-top chamber experiment, membrane lipid and secondary metabolite concentrations exhibited effects of O_3 exposure though no negative effects on whole-plant biomass accumulation were evident. This suggests that, for the limited time window used in our experiment, leaf senescence and secondary metabolite content may be affected at lower levels of O_3 uptake than is growth. Experiments previously conducted to determine the chronic response of plants to accumulated exposure of O_3 have used inhibition of growth and/or photosynthesis as the metric of response, and significant inhibition was found to occur with accumulated exposure over thresholds of 30 or 40 ppb (AOT30 or AOT40) (reviewed by Fuhrer et al., 1997; Skarby et al., 1998; Karlsson et al., 2004). Neither exposure-response nor uptake-response relationships between O_3 and secondary metabolite synthesis have been experimentally determined for any plant. It is also recognized that accumulated exposure to O_3 represents a somewhat arbitrary threshold; other approaches take into account stomatal conductance and estimated O_3 flux into the leaf (Ashmore, 2005; Mills et al., 2011b; Anav et al., 2016).

Evaluating the dose-response relationship for O_3 and secondary metabolite synthesis in tropical as well as temperate plants will be a crucial step towards understanding the ecological effects of O_3 beyond its effects on plant productivity. In particular, the higher solar load and potentially higher leaf temperatures of canopy leaves may result in very different sensitivities of tropical plants. Further, identifying stomatal flux-based relationships between O_3 and carbon assimilation and allocation in tropical species will provide insight into the potential current and future impacts of O_3 on tropical productivity. Although ambient ozone did not decrease growth in our experiment, the duration of the experiment may not have been sufficient to assess an effect on growth. With the

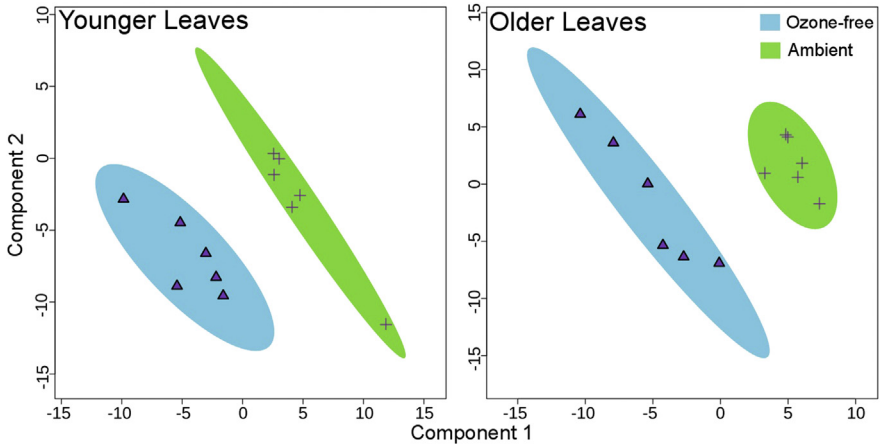

Fig. 4. Results of partial least-squares discriminant analyses of intermediate polarity fractions. Shaded areas represent 95% confidence intervals for combined chromatographic and mass spectral properties of constituents of fractions from each ozone treatment. Each symbol represents one *F. insipida* individual. For younger leaves, component 1 and component 2 accounted for 26.8% and 12.9% of variation respectively. For older leaves, component 1 and component 2 accounted for 25.5% and 13.3% of variation respectively. n = 6 plants.

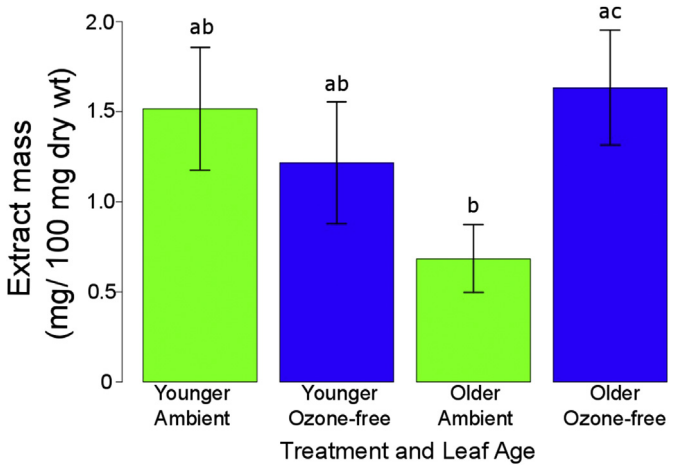

Fig. 5. Gravimetric comparison of nonpolar extracts from *Ficus insipida* leaves across treatments and leaf ontogeny. Error bars indicate ± 1 SEM. Unshared letters above bars indicate significant differences at $P < 0.05$. n = 6 plants.

prospect of large future increases in population in tropical countries, expanding urbanization (Harding et al., 2014), and thus increases in NO_x emissions, together with land cover changes promoting fast growing, high VOC emitting species, e.g. for biofuels (Hewitt et al., 2009), tropical countries face deterioration in air quality. Thus, tropical plant species that exhibit no response or a low-level response to current ambient concentrations of O_3 may be subjected to exposure levels at which carbon assimilation and allocation are impeded. In addition, identifying the occurrence and extent of ozone-induced leaf senescence across a range of tropical tree species will further elucidate the ramifications of elevated [O_3] for tropical forest primary productivity and carbon cycling.

Given that stomatal conductances of tropical trees vary up to 8-fold when the effects of canopy vs. understory and species are combined and up to 4-fold within a stratum (Pearcy, 1987; Roberts et al., 1990; Zotz and Winter 1996; Poorter and Bongers, 2006), the sensitivity of tropical trees will likely differ greatly across species if the correlation between stomatal conductance and sensitivity to O_3 exposure that has been established for temperate trees (Mills et al., 2011a,b; Büker et al., 2015) holds for tropical trees. Thus, it will be important to evaluate the O_3 sensitivity of tropical species representing the full spectrum of stomatal conductances. This will also contribute to an understanding of the ecological effects of O_3 pollution in tropical systems. As the community structure of tropical forests is thought to be tightly intertwined with plant–pest interactions (Coley and Barone, 1996; Coley and Kursar, 2014; Forister et al., 2015; Becerra, 2015) elucidating the extent to which O_3 exposure effects on secondary metabolite synthesis differ among co-occurring plant species will be critical to evaluating and mitigating the effects of O_3 pollution on tropical forests.

Table 4
Putative compounds from UPLC-MS analysis of the combined nonpolar fraction (100% MeOH and 100% ACN) which exhibited significant ($P < 0.05$), ≥1.5-fold changes in concentration between treatments in older leaves. The tentative molecular formulas here reported were assigned based on <10 ppm matches in the METLIN metabolite database and subsequent >90% probability matches in MassHunter software. Putative compounds for which this process did not yield matches are labeled "n/a". A negative fold-change indicates a lower concentration in the ambient vs. the ozone-free treatment. *m/z* indicates the ratio of the mass of the ion in daltons to the total number of charges. $[M+H]^+$ indicates that all of the observed ions were the protonated molecule and have a charge of +1. n = 6 plants.

m/z ($[M+H]^+$)	*P*-value	Fold-change	Predicted molecular formula	Classification of compound
566.491	0.0001	−3.57	$C_{35}H_{66}O_5$	Diglyceride
587.463	0.001	−2.33	$C_{37}H_{62}O_5$	Diglyceride
591.495	0.045	−1.85	$C_{37}H_{66}O_5$	Diglyceride
613.481	0.010	−1.52	$C_{39}H_{64}O_5$	Diglyceride
732.560	0.037	−1.52	n/a	n/a
748.514	0.001	−2.50	$C_{43}H_{72}O_{10}$	n/a
751.535	0.001	−1.89	n/a	n/a
775.540	0.025	2.41	$C_{45}H_{74}O_{10}$	Galactolipid
829.503	0.001	−2.56	n/a	n/a
953.580	0.009	−2.13	n/a	n/a

Acknowledgements

We thank Dr. Phyllis D. Coley, Dr. James Ruff, and three anonymous reviewers for valuable comments on the manuscript. We thank Dr. James Cox, Alan Maschek, and Dale Forrister for assistance with UPLC-MS^2 analysis. We thank Jorge Aranda for assistance with the open-top chamber experiment and Milton Garcia for assistance with the ozone monitoring at the Santa Cruz facility. The authors declare no conflicts of interest. This research was supported by the U.S. Environmental Protection Agency (STAR Fellowship F13F31245), the U.S. National Science Foundation (DEB-1135733, DEB-1405637), the University of Utah's Global Change and Sustainability Center, and the Smithsonian Tropical Research Institute.

Appendix A. Supplementary data

Supplementary data related to this article can be found at http://dx.doi.org/10.1016/j.chemosphere.2016.12.109.

References

Ainsworth, E.A., Yendrek, C.R., Sitch, S., Collins, W.J., Emberson, L.D., 2012. The effects of tropospheric ozone on net primary productivity and implications for climate change. Annu. Rev. Plant Biol. 63, 637–661.
Allen, F., Greiner, R., Wishart, D., 2015. Competitive fragmentation modeling of ESI-MS/MS spectra for putative metabolite identification. Metabolomics 11, 98–110.
Anav, A., De Marco, A., Proietti, C., et al., 2016. Comparing concentration-based (AOT40) and stomatal uptake (PODY) metrics for ozone risk assessment to European forests. Glob. Change Biol. 22, 1608–1627.
Andreae, M.O., Artaxo, P., Brandao, C., et al., 2002. Biogeochemical cycling of carbon, water, energy, trace gases, and aerosols in Amazonia: the LBA-EUSTACH experiments. J. Geophys. Res. 107.
Andreae, M.O., Acevedo, O.C., Araùjo, A., et al., 2015. The Amazon Tall Tower Observatory (ATTO): overview of pilot measurements on ecosystem ecology, meteorology, trace gases, and aerosols. Atmos. Chem. Phys. 15, 10723–10776.
Ashmore, M.R., 2005. Assessing the future global impacts of ozone on vegetation. Plant, Cell Environ. 28, 949–964.
Assis, P.I.L.S., Alonso, R., Meirelles, S.T., Moraes, R.M., 2015. DO3SE model applicability and O3 flux performance compared to AOT40 for an O3-sensitive tropical tree species (Psidium guajava L. "Paluma"). Environ. Sci. Pollut. Res. 22, 10873–10881.
Bakwin, P.S., Wofsy, S.C., Fan, S., 1990. Measurements of reactive nitrogen oxides (NOy) within and above a tropical forest canopy in the wet season. J. Geophys. Res. 95, 16765–16772.
Becerra, J.X., 2015. On the factors that promote the diversity of herbivorous insects and plants in tropical forests. Proc. Natl. Acad. Sci. U. S. A. 112, 6098–6103.
Benton, P., Want, E.J., Ebbels, T.M.D., 2010. Correction of mass calibration gaps in liquid chromatography–mass spectrometry metabolomics data. Bioinformatics 26, 2488–2489.
Bidart-Bouzat, M.G., Imeh-Nathaniel, A., 2008. Global change effects on plant chemical defenses against insect herbivores. J. Integr. Plant Biol. 50, 1339–1354.
Büker, P., Feng, Z., Uddling, J., et al., 2015. New flux based dose-response relationships for ozone for European forest tree species. Environ. Pollut. 206, 163–174.
Cassimiro, J.C., Moraes, R.M., 2016. Responses of a tropical tree species to ozone: visible leaf injury, growth, and lipid peroxidation. Environ. Sci. Pollut. Res. 23, 8085–8090.
Cernusak, L.A., Winter, K., Aranda, J., Turner, B.L., Marshall, J.D., 2007. Transpiration efficiency of a tropical pioneer tree (*Ficus insipida*) in relation to soil fertility. J. Exp. Bot. 58, 3549–3566.
Chappelka, A.H., Samuelson, L.J., 1998. Ambient ozone effects on forest trees of the eastern United States : a review. New Phytol. 139, 91–108.
Coley, P.D., Barone, J.A., 1996. Herbivory and plant defenses in tropical forests. Annu. Rev. Ecol. Syst. 27, 305–335.
Coley, P.D., Kursar, T.A., 2014. On tropical forests and their pests. Science 343, 35–36.
Cros, B., Fontal, J., Minga, A., et al., 1992. Vertical profiles of ozone between 0 meters and 400 meters in and above the African equatorial forest. J. Geophys. Res. Atm. 97, 12877–12887.
Cros, B., Delon, C., Affre, C., Marion, T., Druilhet, A., Perros, P., Lopez, A., 2000. Sources and sinks of ozone in savanna and forest areas during EXPRESSO: airborne turbulent flux measurements. J. Geophys. Res. 105, 347–358.
Crutzen, P.J., Andreae, M., 1990. Biomass burning in the tropics : impact on atmospheric chemistry and biogeochemical cycles. Science 250, 1669–1678.
Emmons, L.K., Walters, S., Hess, P.G., et al., 2010. Description and evaluation of the model for ozone and related chemical tracers, version 4 (MOZART-4). Geosci. Model Dev. 3, 43–67.
Fan, S.M., Wofsy, S.C., Bakwin, P.S., et al., 1990. Atmosphere-biosphere exchange of CO_2 and O_3 in the central Amazon forest. J. Geophys. Res. 95, 16851–16864.
Forister, M.L., Novotny, V., Panorska, A.K., et al., 2015. The global distribution of diet breadth in insect herbivores. Proc. Natl. Acad. Sci. U. S. A. 112, 442–447.
Fishman, J., Wozniak, A.E., Creilson, J.K., 2003. Global distribution of tropospheric ozone from satellite measurements using the empirically corrected tropospheric ozone residual technique: identification of the regional aspects of air pollution. Atmos. Chem. Phys. Discuss. 3, 1453–1476.
Fowler, D., Cape, J.N., Coyle, M., et al., 1999. The global exposure of forests to air pollutants. Water Air Soil Pollut. 116, 5–32.
Fuhrer, J., Skärby, L., Ashmore, M.R., 1997. Critical levels for ozone effects on vegetation in Europe. Environ. Pollut. 97, 91–106.
Furlan, C.M., Moraes, R.M., Bulbovas, P., Sanz, M.J., Domingos, M., Salatino, A., 2008. Tibouchina pulchra (Cham.) Cogn., a native Atlantic Forest species, as a bioindicator of ozone: visible injury. Environ. Pollut. 152, 361–365.
Gerken, T., Wei, D., Chase, R.J., et al., 2016. Downward transport of ozone rich air and implications for atmospheric chemistry in the Amazon rainforest. Atmos. Environ. 124, 64–76.
Gut, A., Scheibe, M., Rottenberger, S., et al., 2002. Exchange fluxes of NO_2 and O_3 at soil and leaf surfaces in an Amazonian rain forest. J. Geophys. Res. 107.
Harding, S., McComiskie, R., Wolff, M., Trewin, D., Hunter, S., 2014. State of the tropics, p. 245.
Hewitt, C.N., MacKenzie, A.R., Di Carlo, P., et al., 2009. Nitrogen management is essential to prevent tropical oil palm plantations from causing ground-level ozone pollution. Proc. Natl. Acad. Sci. U. S. A. 106, 18447–18451.
Hietz, P., Turner, B.L., Wanek, W., Richter, A., Nock, C.A., Wright, S.J., 2011. Long-term change in the nitrogen cycle of tropical forests. Science 334, 664–666.
Hopia, A., Heinonen, M., 1999. Antioxidant activity of flavonol aglycones and their glycosides in methyl linoleate. J. Am. Oil Chem. Soc. 76, 139–144.
Jacob, D.J., Heikes, E.G., Fan, S.-M., et al., 1996. Origin of ozone and NOx in the tropical troposphere: a photochemical analysis of aircraft observations over the South Atlantic basin. J. Geophys. Res. 101, 24235–24250.
Jacob, D.J., Wofsy, S.C., 1990. Budgets of reactive nitrogen, hydrocarbons, and ozone over the Amazon forest during the wet season. J. Geophys. Res. 95, 16737–16754.
Jardine, K., Yañez Serrano, A., Arneth, A., et al., 2011. Within-canopy sesquiterpene ozonolysis in Amazonia. J. Geophys. Res. 116.
Kangasjärvi, J., Jaspers, P., Kollist, H., 2005. Signalling and cell death in ozone-exposed plants. Plant Cell Environ. 28, 1021–1036.
Kaplan, W.A., Wofsy, S.C., Keller, M., Da Costa, J.M., 1988. Emission of NO and deposition of O_3 in a tropical forest system. J. Geophys. Res. 93, 1389–1395.
Karl, T., Guenther, A., Turnipseed, A., Tyndall, G., Artaxo, P., Martin, S., 2009. Rapid formation of isoprene photo-oxidation products observed in Amazonia. Atmos. Chem. Phys. 9, 7753–7767.
Karlsson, P.E., Uddling, J., Braun, S., et al., 2004. New critical levels for ozone effects on young trees based on AOT40 and simulated cumulative leaf uptake of ozone. Atmos. Environ. 38, 2283–2294.
Karnosky, D.F., Skelly, J.M., Percy, K.E., Chappelka, A.H., 2007. Perspectives regarding 50 years of research on effects of tropospheric ozone air pollution on US forests. Environ. Pollut. 147, 489–506.
Kelliher, F.M., Leuning, R., Raupach, M.R., Schulze, E.D., 1995. Maximum conductances for evaporation from global vegetation types. Agric. For. Meteorol. 73, 1–16.
Kirchhoff, V.W.J.H., da Silva, I.M.O., Browell, E.V., 1990. Ozone measurement in Amazonia: dry season versus wet season. J. Geophys. Res. 95, 16913–16926.
Kopper, B.J., Lindroth, R.L., 2003. Effects of elevated carbon dioxide and ozone on the phytochemistry of aspen and performance of an herbivore. Oecologia 134, 95–103.
Körner, C., 1995. Leaf diffusive conductances in the major vegetation types of the globe. Ecophysiol. Photosynth. 100, 463–490.
Krause, G.H., Gallé, A., Virgo, A., García, M., Bucic, P., Jahns, P., Winter, K., 2006. High-light stress does not impair biomass accumulation of sun-acclimated tropical tree seedlings (*Calophyllum longifolium* Willd. and *Tectona grandis* L. f.). Plant Biol. 8, 31–41.
Krause, G.H., Jahns, P., Virgo, A., García, M., Aranda, J., Wellmann, E., Winter, K., 2007. Photoprotection, photosynthesis and growth of tropical tree seedlings under near-ambient and strongly reduced solar ultraviolet-B radiation. J. Plant Physiol. 164, 1311–1322.
Kuhl, C., Tautenhahn, R., Böttcher, C., Larson, T.R., Neumann, S., 2012. CAMERA: an integrated strategy for compound spectra extraction and annotation of liquid chromatography/mass spectrometry data sets. Anal. Chem. 84, 283–289.
Leigh Jr., E.G., Rand, A.S., Windsor, D.M., 1996. The Ecology of a Tropical Forest: Seasonal Rhythms and Long Term Changes, second ed. Smithsonian Institution Press, Washington, DC.
Lindroth, R.L., 2010. Impacts of elevated atmospheric CO_2 and O_3 on forests: phytochemistry, trophic interactions, and ecosystem dynamics. J. Chem. Ecol. 36, 2–21.
Matsuda, K., Watanabe, I., Wingpud, V., Theramongkol, P., Ohizumi, T., 2006. Deposition velocity of O_3 and SO_2 in the dry and wet season above a tropical forest in northern Thailand. Atmos. Environ. 40, 7557–7564.
Mills, G., Hayes, F., Simpson, D., Emberson, L., Norris, D., Harmens, H., Büker, P., 2011a. Evidence of widespread effects of ozone on crops and (semi-)natural vegetation in Europe (1990-2006) in relation to AOT40- and flux-based risk maps. Glob. Change Biol. 17, 592–613.
Mills, G., Pleijel, H., Braun, S., et al., 2011b. New stomatal flux-based critical levels for ozone effects on vegetation. Atmos. Environ. 45, 5064–5068.

Mishra, S., Tyagi, A., Singh, I.V., Sangwan, R.S., 2006. Changes in lipid profile during growth and senescence of Catharanthus roseus leaf. Braz. J. Plant Physiol. 18, 447–454.
Musselman, R.C., Lefohn, A.S., Massman, W.J., Heath, R.L., 2006. A critical review and analysis of the use of exposure- and flux-based ozone indices for predicting vegetation effects. Atmos. Environ. 40, 1869–1888.
Naik, V., Voulgarakis, A., Fiore, A.M., et al., 2013. Preindustrial to present-day changes in tropospheric hydroxyl radical and methane lifetime from the Atmospheric Chemistry and Climate Model Intercomparison Project (ACCMIP). Atmos. Chem. Phys. 13, 5277–5298.
Pacifico, F., Folberth, G.A., Sitch, S., Haywood, J.M., Artaxo, P., Malavelle, F.F., Rizzo, L.V., 2015. Biomass burning related ozone damage on vegetation over the Amazon forest. Atmos. Chem. Phys. 15, 2791–2804.
Pearcy, R., 1987. Photosynthetic gas exchange responses of Australian tropical forest trees in canopy, gap and understory micro-environments. Funct. Ecol. 1, 169–178.
Poorter, L., Bongers, F., 2006. Leaf traits are good predictors of plant performance across 53 rain forest species. Ecology 87, 1733–1743.
R Core Team, 2015. R: a Language and Environment for Statistical Computing. R Foundation for Statistical Computing, Vienna, Austria.
Roberts, J., Cabral, O.M.R., De Aguiar, L.F., 1990. Stomatal and boundary-layer conductances in an Amazonian terra firme rain forest. J. Appl. Ecol. 27, 336–353.
Rummel, U., Ammann, C., Kirkman, G.A., et al., 2007. Seasonal variation of ozone deposition to a tropical rain forest in southwest Amazonia. Atmos. Chem. Phys. 7, 5415–5435.
Sandermann Jr., H., 1996. Ozone and plant health. Annu. Rev. Phytopathol. 34, 347–366.
Simon, E.W., 1974. Phospholipids and plant membrane permeability. New Phytol. 73, 377–420.
Sitch, S., Cox, P.M., Collins, W.J., Huntingford, C., 2007. Indirect radiative forcing of climate change through ozone effects on the land-carbon sink. Nature 448, 791–794.
Skarby, L., Ro-Poulsen, H., Wellburn, F.A.M., Sheppard, L.J., 1998. Impacts of ozone on forests : a European perspective. New Phytol. 109–122.
Smith, C.A., Want, E.J., O'Maille, G., Abagyan, R., Siuzdak, G., 2006. XCMS: processing mass spectrometry data for metabolite profiling using nonlinear peak alignment, matching, and identification. Anal. Chem. 78, 779–787.
STRI Physical Monitoring Program. (Accessed 12 October 2016). http://biogeodb.stri.si.edu/physical_monitoring/research/metpark.
Tautenhahn, R., Böttcher, C., Neumann, S., 2008. Highly sensitive feature detection for high resolution LC/MS. BMC Bioinforma. 9, 504.
Tropicos.org, 01 May 2016. Missouri Botanical Garden. http://www.tropicos.org/Name/21300606.
Valkama, E., Koricheva, J., Oksanen, E., 2007. Effects of elevated O_3, alone and in combination with elevated CO_2, on tree leaf chemistry and insect herbivore performance: a meta-analysis. Glob. Change Biol. 13, 184–201.
Vingarzan, R., 2004. A review of surface ozone background levels and trends. Atmos. Environ. 38, 3431–3442.
Wiggins, N.L., Forrister, D.L., Endara, M.-J., Coley, P.D., Kursar, T.A., 2016. Quantitative and qualitative shifts in defensive metabolites define chemical defense investment during leaf development in *Inga*, a genus of tropical trees. Ecol. Evol. 6, 478–492.
Wild, O., Fiore, A.M., Shindell, D.T., et al., 2012. Modelling future changes in surface ozone: a parameterized approach. Atmos. Chem. Phys. 12, 2037–2054.
Wittig, V.E., Ainsworth, E.A., Naidu, S.L., Karnosky, D.F., Long, S.P., 2009. Quantifying the impact of current and future tropospheric ozone on tree biomass, growth, physiology and biochemistry: a quantitative meta-analysis. Glob. Change Biol. 15, 396–424.
Xia, J., Sinelnikov, I., Han, B., Wishart, D.S., 2015. MetaboAnalyst 3.0 – making metabolomics more meaningful. Nucleic Acids Res. 43, W251–W257.
Yang, Z., Ohlrogge, J.B., 2009. Turnover of fatty acids during natural senescence of Arabidopsis, Brachypodium, and switchgrass and in Arabidopsis beta-oxidation mutants. Plant Physiol. 150, 1981–1989.
Zotz, G., Harris, G., Königer, M., Winter, K., 1995. High rates of photosynthesis in a tropical pioneer tree. Ficus Insipida. Flora 190, 265–272.
Zotz, G., Winter, K., 1996. Diel patterns of CO2 exchange in rainforest canopy plants. In: Mulkey, S.S., Chazdon, R.L., Smith, A.P. (Eds.), Tropical Forest Plant Ecophysiology. Chapman and Hall, New York, pp. 89–113.